



Multicaloric and coupled-caloric effects

Jia-Zheng Hao(郝嘉政), Feng-Xia Hu(胡凤霞), Zi-Bing Yu(尉紫冰), Fei-Ran Shen(沈斐然), Hou-Bo Zhou(周厚博), Yi-Hong Gao(高怡红), Kai-Ming Qiao(乔凯明), Jia Li(李佳), Cheng Zhang(张丞), Wen-Hui Liang(梁文会), Jing Wang(王晶), Jun He(何峻), Ji-Rong Sun(孙继荣), Bao-Gen Shen(沈保根)

Citation: Chin. Phys. B . 2020, 29(4): 047504 . doi: 10.1088/1674-1056/ab7da7

Journal homepage: <http://cpb.iphy.ac.cn>; <http://iopscience.iop.org/cpb>

What follows is a list of articles you may be interested in

Giant low-field magnetocaloric effect in $\text{EuTi}_{1-x}\text{Nb}_x\text{O}_3$ ($x=0.05, 0.1, 0.15$, and 0.2) compounds

Wen-Hao Jiang(姜文昊), Zhao-Jun Mo(莫兆军), Jia-Wei Luo(罗佳薇), Zhe-Xuan Zheng(郑哲轩), Qiu-Jie Lu(卢秋杰), Guo-Dong Liu(刘国栋), Jun Shen(沈俊), Lan Li(李岚)

Chin. Phys. B . 2020, 29(3): 037502 . doi: 10.1088/1674-1056/ab69e7

Magneto-resistance hysteresis in topological Kondo insulator SmB_6 nanowire

Ling-Jian Kong(孔令剑), Yong Zhou(周勇), Hua-Ding Song(宋化鼎), Da-Peng Yu(俞大鹏), Zhi-Min Liao(廖志敏)

Chin. Phys. B . 2019, 28(10): 107501 . doi: 10.1088/1674-1056/ab3a89

Critical behavior and magnetocaloric effect in magnetic Weyl semimetal candidate $\text{Co}_{2-x}\text{ZrSn}$

Tianlin Yu(于天麟), Xiaoyun Yu(余骁昀), En Yang(杨恩), Chang Sun(孙畅), Xiao Zhang(张晓), Ming Lei(雷鸣)

Chin. Phys. B . 2019, 28(6): 067501 . doi: 10.1088/1674-1056/28/6/067501

Magnetic properties and magnetocaloric effects in $(\text{Ho}_{1-x}\text{Y}_x)_5\text{Pd}_2$ compounds

X F Wu(武小飞), C P Guo(郭翠萍), G Cheng(成钢), C R Li(李长荣), J Wang(王江), Y S Du(杜玉松), G H Rao(饶光辉), Z M Du(杜振民)

Chin. Phys. B . 2019, 28(5): 057502 . doi: 10.1088/1674-1056/28/5/057502

Ferromagnetism and magnetostructural coupling in V-doped MnNiGe alloys

Hui Yang(杨慧), Jun Liu(刘俊), Chao Li(李超), Guang-Long Wang(王广龙), Yuan-Yuan Gong(龚元元), Feng Xu(徐锋)

Chin. Phys. B . 2018, 27(10): 107502 . doi: 10.1088/1674-1056/27/10/107502

1055-0748 — 中国物理 B

CPB

Chinese Physics B

Volume 29 April 2020 Number 4

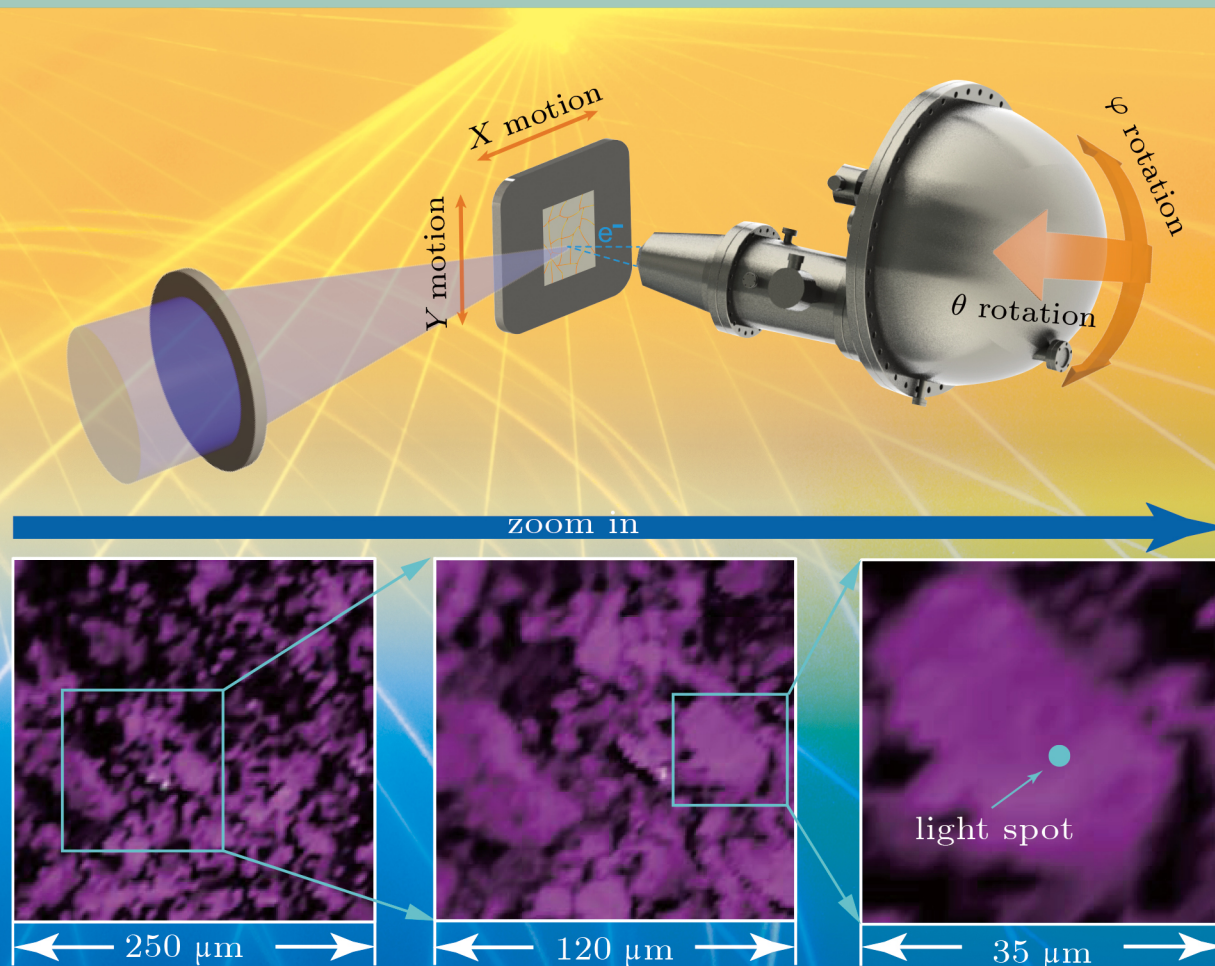
TOPICAL REVIEW

- Physics in neuromorphic devices
- Magnetism, magnetic materials, and interdisciplinary research

SPECIAL TOPIC

- Advanced calculation & characterization of energy storage materials & devices at multiple scale
- Ion beam technology
- Optical field manipulation
- Terahertz physics

A series Journal of the Chinese Physical Society Distributed by IOP Publishing

iopscience.org/cpb | cpb.iphy.ac.cn
**Featured Article**

Electronic structure and spatial inhomogeneity of iron-based superconductor FeS

Chengwei Wang, Meixiao Wang, Juan Jiang, Haifeng Yang, Lexian Yang, Wujun Shi, Xiaofang Lai,

Sung-Kwan Mo, Alexei Barinov, Binghai Yan, Zhi Liu, Fuqiang Huang, Jinfeng Jia, Zhongkai Liu and Yulin Chen

Chin. Phys. B, 2020, 29(4): 047401

Chinese Physics B (中国物理 B)

Published monthly in hard copy by the Chinese Physical Society and online by IOP Publishing, Temple Circus, Temple Way, Bristol BS1 6HG, UK

Institutional subscription information: 2020 volume

For all countries, except the United States, Canada and Central and South America, the subscription rate per annual volume is UK £1326 (electronic only) or UK £1446 (print + electronic).

Delivery is by air-speeded mail from the United Kingdom.

Orders to:

Journals Subscription Fulfilment, IOP Publishing, Temple Circus, Temple Way, Bristol BS1 6HG, UK

For the United States, Canada and Central and South America, the subscription rate per annual volume is US\$2640 (electronic only) or US\$2870 (print + electronic). Delivery is by transatlantic airfreight and onward mailing.

Orders to: IOP Publishing, P. O. Box 320, Congers, NY 10920-0320, USA

© 2020 Chinese Physical Society and IOP Publishing Ltd

All rights reserved. No part of this publication may be reproduced, stored in a retrieval system, or transmitted in any form or by any means, electronic, mechanical, photocopying, recording or otherwise, without the prior written permission of the copyright owner.

Supported by the China Association for Science and Technology and Chinese Academy of Sciences

Editorial Office: Institute of Physics, Chinese Academy of Sciences, P. O. Box 603, Beijing 100190, China
Tel: (86-10) 82649026 or 82649519, Fax: (86-10) 82649027, E-mail: cpb@aphy.iphy.ac.cn

主管单位: 中国科学院

国际统一刊号: ISSN 1674-1056

主办单位: 中国物理学会和中国科学院物理研究所

国内统一刊号: CN 11-5639/O4

主 编: 欧阳钟灿

编辑部地址: 北京 中关村 中国科学院物理研究所内

出 版: 中国物理学会

通 讯 地 址: 100190 北京 603 信箱

印刷装订: 北京科信印刷有限公司

电 话: (010) 82649026, 82649519

编 辑: Chinese Physics B 编辑部

传 真: (010) 82649027

国内发行: Chinese Physics B 出版发行部

“Chinese Physics B”网址:

国外发行: IOP Publishing Ltd

<http://cpb.iphy.ac.cn>

发行范围: 公开发行

<http://iopscience.iop.org/journal/1674-1056>

Published by the Chinese Physical Society

Advisory Board

Prof. Academician Chen Jia-Er(陈佳洱)

School of Physics, Peking University, Beijing 100871, China

Prof. Academician Feng Duan(冯端)

Department of Physics, Nanjing University, Nanjing 210093, China

Prof. Academician T. D. Lee(李政道)

Department of Physics, Columbia University, New York, NY 10027, USA

Prof. Academician Samuel C. C. Ting(丁肇中)

LEP3, CERN, CH-1211, Geneva 23, Switzerland

Prof. Academician C. N. Yang(杨振宁)

Institute for Theoretical Physics, State University of New York, USA

Prof. Academician Yang Fu-Jia(杨福家)

Department of Nuclear Physics, Fudan University, Shanghai 200433, China

Prof. Academician Zhou Guang-Zhao
(Chou Kuang-Chao)(周光召)

China Association for Science and Technology, Beijing 100863, China

Prof. Academician Wang Nai-Yan(王乃彦)

China Institute of Atomic Energy, Beijing 102413, China

Editor-in-Chief

Prof. Academician Ouyang Zhong-Can(欧阳钟灿)

Institute of Theoretical Physics, Chinese Academy of Sciences, Beijing 100190, China

Associate Editors

- Prof. Academician Zhao Zhong-Xian(赵忠贤) Institute of Physics, Chinese Academy of Sciences, Beijing 100190, China
Prof. Academician Yang Guo-Zhen(杨国桢) Institute of Physics, Chinese Academy of Sciences, Beijing 100190, China
Prof. Academician Zhang Jie(张杰) Chinese Academy of Sciences, Beijing 100864, China
Prof. Academician Xing Ding-Yu(邢定钰) Department of Physics, Nanjing University, Nanjing 210093, China
Prof. Academician Shen Bao-Gen(沈保根) Institute of Physics, Chinese Academy of Sciences, Beijing 100190, China
Prof. Academician Gong Qi-Huang(龚旗煌) School of Physics, Peking University, Beijing 100871, China
Prof. Academician Xue Qi-Kun(薛其坤) Department of Physics, Tsinghua University, Beijing 100084, China
Prof. Sheng Ping(沈平) The Hong Kong University of Science & Technology, Kowloon, Hong Kong, China

Editorial Board

- Prof. David Andelman School of Physics and Astronomy Tel Aviv University, Tel Aviv 69978, Israel
Prof. Academician Chen Xian-Hui(陈仙辉) Department of Physics, University of Science and Technology of China, Hefei 230026, China
Prof. Cheng Jian-Chun(程建春) School of Physics, Nanjing University, Nanjing 210093, China
Prof. Chia-Ling Chien Department of Physics and Astronomy, The Johns Hopkins University, Baltimore, MD 21218, USA
Prof. Dai Xi(戴希) Institute of Physics, Chinese Academy of Sciences, Beijing 100190, China
Prof. Ding Jun(丁军) Department of Materials Science & Engineering, National University of Singapore, Singapore 117576, Singapore
Prof. Masao Doi Toyota Physical and Chemical Research Institute, Yokomichi, Nagakute, Aichi 480-1192, Japan
Prof. Fang Zhong(方忠) Institute of Physics, Chinese Academy of Sciences, Beijing 100190, China
Prof. Feng Shi-Ping(冯世平) Department of Physics, Beijing Normal University, Beijing 100875, China
Prof. Academician Gao Hong-Jun(高鸿钧) Institute of Physics, Chinese Academy of Sciences, Beijing 100190, China
Prof. Gu Chang-Zhi(顾长志) Institute of Physics, Chinese Academy of Sciences, Beijing 100190, China
Prof. Gu Min(顾敏) School of Optical-Electrical and Computer Engineering, University of Shanghai for Science and Technology, Shanghai 200093, China
Prof. Academician Guo Guang-Can(郭光灿) School of Physical Sciences, University of Science and Technology of China, Hefei 230026, China
Prof. Academician He Xian-Tu(贺贤土) Institute of Applied Physics and Computational Mathematics, Beijing 100088, China
Prof. Werner A. Hofer Stephenson Institute for Renewable Energy, The University of Liverpool, Liverpool L69 3BX, UK
Prof. Hong Ming-Hui(洪明辉) Department of Electrical and Computer Engineering, National University of Singapore, Singapore 117576, Singapore
Prof. Hu Gang(胡岗) Department of Physics, Beijing Normal University, Beijing 100875, China
Prof. Jiang Hong-Wen(姜弘文) Department of Physics and Astronomy, University of California, Los Angeles, CA 90095, USA
Prof. Jiang Ying(江颖) School of Physics, Peking University, Beijing 100871, China
Prof. Jin Xiao-Feng(金晓峰) Department of Physics, Fudan University, Shanghai 200433, China
Prof. Robert J. Joynt Physics Department, University of Wisconsin-Madison, Madison, USA
Prof. Jaewan Kim Korea Institute for Advanced Study, School of Computational Sciences, Hoegiro 85, Seoul 02455, Korea
Prof. Li Ru-Xin(李儒新) Shanghai Institute of Optics and Fine Mechanics, Chinese Academy of Sciences, Shanghai 201800, China
Prof. Li Xiao-Guang(李晓光) Department of Physics, University of Science and Technology of China, Hefei 230026, China
Assits. Prof. Liu Chao-Xing(刘朝星) Department of Physics, Pennsylvania State University, PA 16802-6300, USA
Prof. Liu Xiang-Yang(刘向阳) Department of Physics, Xiamen University, Xiamen 361005, China
Prof. Liu Ying(刘荧) Department of Physics and Astronomy, Shanghai Jiao Tong University, Shanghai 200240, China
Prof. Long Gui-Lu(龙桂鲁) Department of Physics, Tsinghua University, Beijing 100084, China
Prof. Lv Li(吕力) Institute of Physics, Chinese Academy of Sciences, Beijing 100190, China
Prof. Ma Xu-Cun(马旭村) Department of Physics, Tsinghua University, Beijing 100084, China
Prof. Antonio H. Castro Neto Physics Department, Faculty of Science, National University of Singapore, Singapore 117546, Singapore
Prof. Nie Yu-Xin(聂玉昕) Institute of Physics, Chinese Academy of Sciences, Beijing 100190, China
Prof. Niu Qian(牛谦) Department of Physics, University of Texas, Austin, TX 78712, USA
Prof. Academician Ouyang Qi(欧阳颀) School of Physics, Peking University, Beijing 100871, China

- Prof. Academician Pan Jian-Wei(潘建伟) Department of Modern Physics, University of Science and Technology of China, Hefei 230026, China
- Prof. Amalia Patane School of Physics and Astronomy, The University of Nottingham, NG7 2RD, UK
- Prof. Qian Lie-Jia(钱列加) Department of Physics and Astronomy, Shanghai Jiao Tong University, Shanghai 200240, China
- Prof. J. Y. Rhee Department of Physics, Sungkyunkwan University, Suwon, Korea
- Prof. Shen Jian(沈健) Department of Physics, Fudan University, Shanghai 200433, China
- Prof. Shen Yuan-Rang(沈元壤) Lawrence Berkeley National Laboratory, Berkeley, CA 94720, USA
- Prof. Shen Zhi-Xun(沈志勋) Stanford University, Stanford, CA 94305-4045, USA
- Prof. Academician Sun Chang-Pu(孙昌璞) Beijing Computational Science Research Center, China Academy of Engineering Physics, Beijing 100094, China
- Prof. Sun Xiao-Wei(孙小卫) Department of Electrical and Electronic Engineering, Southern University of Science and Technology, Shenzhen 518055, China
- Prof. Sun Xiu-Dong(孙秀冬) Department of Physics, Harbin Institute of Technology, Harbin 150001, China
- Prof. Michiyoshi Tanaka Research Institute for Scientific Measurements, Tohoku University, Katahira 2-1-1, Aoba-ku 980, Sendai, Japan
- Prof. Tong Li-Min(童利民) Department of Optical Engineering, Zhejiang University, Hangzhou 310027, China
- Prof. Tong Peng'er(童彭尔) Department of Physics, The Hong Kong University of Science and Technology, Kowloon, Hong Kong, China
- Prof. Wang Bo-Gen(王伯根) School of Physics, Nanjing University, Nanjing 210093, China
- Prof. Wang Kai-You(王开友) Institute of Semiconductors, Chinese Academy of Sciences, Beijing 100083, China
- Prof. Wang Wei(王炜) School of Physics, Nanjing University, Nanjing 210093, China
- Prof. Wang Ya-Yu(王亚愚) Department of Physics, Tsinghua University, Beijing 100084, China
- Prof. Wang Yu-Peng(王玉鹏) Institute of Physics, Chinese Academy of Sciences, Beijing 100190, China
- Prof. Wang Zhao-Zhong(王肇中) Laboratory for Photonics and Nanostructures (LPN) CNRS-UPR20, Route de Nozay, 91460 Marcoussis, France
- Prof. Academician Wang Wei-Hua(汪卫华) Institute of Physics, Chinese Academy of Sciences, Beijing 100190, China
- Prof. Wei Su-Huai(魏苏淮) Beijing Computational Science Research Center, China Academy of Engineering Physics, Beijing 100094, China
- Prof. Wen Hai-Hu(闻海虎) Department of Physics, Nanjing University, Nanjing 210093, China
- Prof. Wu Nan-Jian(吴南健) Institute of Semiconductors, Chinese Academy of Sciences, Beijing 100083, China
- Prof. Academician Xia Jian-Bai(夏建白) Institute of Semiconductors, Chinese Academy of Sciences, Beijing 100083, China
- Prof. Academician Xiang Tao(向涛) Institute of Physics, Chinese Academy of Sciences, Beijing 100190, China
- Prof. Academician Xie Si-Shen(解思深) Institute of Physics, Chinese Academy of Sciences, Beijing 100190, China
- Prof. Academician Xie Xin-Cheng(谢心澄) Department of Physics, Peking University, Beijing 100871, China
- Prof. Academician Xu Zhi-Zhan(徐至展) Shanghai Institute of Optics and Fine Mechanics, Chinese Academy of Sciences, Shanghai 201800, China
- Assist. Prof. Xu Cen-Ke(许岑珂) Department of Physics, University of California, Santa Barbara, CA 93106, USA
- Prof. Academician Ye Chao-Hui(叶朝辉) Wuhan Institute of Physics and Mathematics, Chinese Academy of Sciences, Wuhan 430071, China
- Prof. Ye Jun(叶军) Department of Physics, University of Colorado, Boulder, Colorado 80309-0440, USA
- Prof. Yu Ming-Yang(郁明阳) Theoretical Physics I, Ruhr University, D-44780 Bochum, Germany
- Prof. Academician Zhan Wen-Long(詹文龙) Chinese Academy of Sciences, Beijing 100864, China
- Prof. Zhang Fu-Chun(张富春) Kavli Institute for Theoretical Sciences, University of Chinese Academy of Sciences, Beijing 100190, China
- Prof. Zhang Xiang(张翔) NSF Nanoscale Science and Engineering Center (NSEC), University of California, Berkeley, CA 94720, USA
- Prof. Zhang Yong(张勇) Electrical and Computer Engineering Department, The University of North Carolina at Charlotte, Charlotte, USA
- Prof. Zhang Zhen-Yu(张振宇) International Center for Quantum Design of Functional Materials, University of Science and Technology of China, Hefei 230026, China
- Prof. Zeng Hao(曾浩) Department of Physics, University at Buffalo, SUNY, Buffalo, NY 14260, USA
- Prof. Zheng Bo(郑波) Physics Department, Zhejiang University, Hangzhou 310027, China
- Prof. Zhou Xing-Jiang(周兴江) Institute of Physics, Chinese Academy of Sciences, Beijing 100190, China
- Prof. Academician Zhu Bang-Fen(朱邦芬) Department of Physics, Tsinghua University, Beijing 100084, China

Editorial Staff

Wang Jiu-Li(王久丽) (Editorial Director) Cai Jian-Wei(蔡建伟) Zhai Zhen(翟振)

Multicaloric and coupled-caloric effects*

Jia-Zheng Hao(郝嘉政)^{1,2}, Feng-Xia Hu(胡凤霞)^{2,3,4,†}, Zi-Bing Yu(尉紫冰)^{2,3}, Fei-Ran Shen(沈斐然)^{2,3},
Hou-Bo Zhou(周厚博)^{2,3}, Yi-Hong Gao(高怡红)^{2,3}, Kai-Ming Qiao(乔凯明)^{2,3}, Jia Li(李佳)^{2,3},
Cheng Zhang(张丞)^{2,3}, Wen-Hui Liang(梁文会)^{2,3}, Jing Wang(王晶)^{2,3,5}, Jun He(何峻)^{1,‡},
Ji-Rong Sun(孙继荣)^{2,3,4}, and Bao-Gen Shen(沈保根)^{2,3,4}

¹Division of Functional Material Research, Central Iron and Steel Research Institute, Beijing 100081, China

²Beijing National Laboratory for Condensed Matter Physics & State Key Laboratory of Magnetism, Institute of Physics, Chinese Academy of Sciences, Beijing 100190, China

³School of Physical Sciences, University of Chinese Academy of Sciences, Beijing 100049, China

⁴Songshan Lake Materials Laboratory, Dongguan 523808, China

⁵Fujian Innovation Academy, Chinese Academy of Sciences, Fuzhou 350108, China

(Received 1 February 2020; revised manuscript received 20 February 2020; accepted manuscript online 9 March 2020)

The multicaloric effect refers to the thermal response of a solid material driven by simultaneous or sequential application of more than one type of external field. For practical applications, the multicaloric effect is a potentially interesting strategy to improve the efficiency of refrigeration devices. Here, the state of the art in multi-field driven multicaloric effect is reviewed. The phenomenology and fundamental thermodynamics of the multicaloric effect are well established. A number of theoretical and experimental research approaches are covered. At present, the theoretical understanding of the multicaloric effect is thorough. However, due to the limitation of the current experimental technology, the experimental approach is still in progress. All these researches indicated that the thermal response and effective reversibility of multiferroic materials can be improved through multicaloric cycles to overcome the inherent limitations of the physical mechanisms behind single-field-induced caloric effects. Finally, the viewpoint of further developments is presented.

Keywords: multicaloric effect, coupled-caloric effect, solid-state refrigeration, magnetocaloric effect

PACS: 05.70.Fh, 65.40.gd, 75.30.Sg, 75.85.+t

DOI: 10.1088/1674-1056/ab7da7

1. Introduction

Solid-state refrigeration technology based on the caloric effects has superior refrigeration efficiency while reducing ozone consumption or greenhouse gas emissions. Therefore, it provides an energy-saving and environmentally-friendly refrigeration solution to replace the current mainstream vapor compression refrigeration technology.^[1–6] The caloric effect of a solid refers to the reversible thermal change (isothermal change of entropy or adiabatic change of temperature) of the solid under the application of an external stimulus field, which generally occurs in the vicinity of phase transitions. The known caloric effects mainly include magnetocaloric effects,^[1–6] electrocaloric effects,^[7] and mechanical caloric effects (barocaloric^[8] and elastocaloric effects^[9]), which correspond to magnetic, electric, and mechanical fields (hydrostatic pressure and uniaxial stress), respectively. Multiferroic materials show two or more ferroic orders, and when the couplings of these ferroic orders are strong enough, each ferroic order can respond to more than one type of applied field.

In addition, multiple ferroic phase transitions may occur at a nearby temperature. Therefore, it is expected that most giant magnetocaloric and electrocaloric materials will also exhibit mechanocaloric effects, since the magnetic and polar orders in such materials are strongly coupled to the lattice order.^[10] The magnetocaloric, electrocaloric, or mechanocaloric effect will directly affect each other due to the cross-response to the magnetic/electric or mechanical field. Some studies have shown that the multicaloric effect driven by multiple fields may yield larger caloric response compared to the caloric effect induced by a single stimulus.^[11–17]

So far, the study of single-field induced solid-state caloric effects has attracted widespread attention. In particular, giant magnetocaloric effects are generally observed when the ferroic phase transition is first order in nature.^[18–27] Many studies have focused on achieving stronger magnetic first-order transitions, that is, achieving the greatest latent heat and the strongest magnetic–structural coupling. This method is beneficial to achieve higher caloric performance, especially large entropy changes. However, it is accompanied by many disad-

*Project supported by the National Key Research and Development Program of China (Grant Nos. 2017YFB0702702, 2019YFA0704904, 2018YFA0305704, 2017YFA0206300, 2017YFA0303601, and 2016YFB0700903), the National Natural Science Foundation of China (Grant Nos. U1832219, 51531008, 51771223, 51590880, 51971240, 11674378, 11934016, and 11921004), and the Key Program and Strategic Priority Research Program (B) of the Chinese Academy of Sciences.

†Corresponding author. E-mail: fxhu@iphy.ac.cn

‡Corresponding author. E-mail: hejun@cisri.com.cn

vantages, such as large hysteresis loss, irreversibility of caloric effects, or poor mechanical stability. These definite drawbacks have limited the practical application and further development of the first-order transition materials in solid-state refrigeration. Considerable efforts have recently been made to overcome these problems.^[28–34] Recent studies indicated that the hysteresis loss of materials can be reduced or even eliminated by utilizing the response of multiferroic materials to more than one type of driving field.^[29,30,32] These studies have led to an enthusiastic search for multicaloric cycle and have encouraged fast-growing research activities in the field. The theoretical framework for multicaloric effect has been studied in sufficient detail.^[16,17,35–37] However, due to the limitation of the current experimental technology, quite few experimental efforts have been devoted to the study of these combined magneto–mechanic or electro–mechanic caloric effects with the coupled term considered.^[15,17,38] At present, most of the reported results involve studies on the effects of mechanical stress on the magnetocaloric and electrocaloric effects, while a small amount focus on the regulation of electro-induced strain on the magnetocaloric effect in magnetostructural coupled materials. Furthermore, cryogenic rare earth-based alloys and intermetallic compounds are mainly second order materials showing considerable magnetocaloric effect (MCE),^[4,5,39–44] such as R - T (R = rare earth element; T = Fe, Co, Ni, Zn, and Ga) compounds,^[5,45–54] ternary RTX (T = Fe, Co, and Pt; X = Al, Mg, and C) compounds,^[55–60] ternary R_2T_2Al (T = Co, Ni, and Cu) and R_2Ni_2In compounds,^[41,61,62] ternary R_4TX (T = Co, Pd, and Pt; X = Mg and Cd) compounds,^[63,64] and quaternary RNi_2B_2C and $RNiBC$ compounds.^[65] However, some of these rare earth-based MCE materials still undergo unneglectable spin–lattice coupling, though the thermal and magnetic hysteresis may be approaching zero. For example, the spin orientation transition is occasionally accompanied by an abnormal lattice change, and a stress can also shift the transition. Because the experimental studies on the multicaloric and coupled-caloric effects are still limited, there are no relative reports involving the rare earth-based MCE materials up to now. Therefore, in this article the review mainly focuses on the multicaloric effect and coupled-caloric effect in the materials with significant characteristics of first-order transition.

In this article, we present a brief review of the state of the art in research on multicaloric materials and multicaloric effects. The phenomenology and fundamental thermodynamics of the multicaloric effect are reviewed, including some common theoretical and experimental approaches to study the multicaloric effect and coupled-caloric effect. Finally, the viewpoint of further developments is presented.

2. Thermodynamics of multicaloric effect

The ferroic material can be characterized by ferroic property X_i with corresponding thermodynamically conjugated field x_i . These pairs of variables can be magnetization M and magnetic field H , polarization P and electric field E , or strain ϵ and stress σ . The caloric effects caused by the finite changes in the field x_i (keeping the remaining fields constant) are usually quantified by the entropy changes that occur when the field is applied or removed isothermally, and the temperature changes that occur when the field undergoes an adiabatic change. The isothermal change of the field-induced entropy can be obtained by integrating the appropriate Maxwell equation^[15,17,36,37]

$$\Delta S(T, 0 \rightarrow x_i) = S(T, x_i) - S(T, 0) = \int_0^{x_i} \left(\frac{\partial X_i}{\partial T} \right)_{x_i} dx_i. \quad (1)$$

When the field is varied adiabatically, the entropy is constant. The adiabatic temperature change can be obtained by the following equation:

$$\Delta T(0 \rightarrow x_i) = T(S, x_i) - T(S, 0) = - \int_0^{x_i} \frac{T}{C} \left(\frac{\partial X_i}{\partial T} \right)_{x_i} dx_i. \quad (2)$$

Multiferroic materials display two or more of the non-independence ferroic properties, and they may be strongly coupled. The multicaloric effects occur when more than one field is either simultaneously or sequentially applied. For the sake of clarity and practical applications, the system is considered with two ferroic properties X_1 and X_2 with thermodynamically conjugated fields x_1 and x_2 , respectively. In general, for adiabatic temperature changes, it is easy to obtain similar expressions to that obtained for isothermal entropy changes. Similar to the caloric effect induced by a single field in an equilibrium thermodynamic system, the multicaloric effect can also be quantified by the isothermal entropy change. Furthermore, the entropy is a state function, so the magnitude of the isothermal entropy change is independent of the thermodynamic path of the applied multiple external fields, and it does not depend on whether the driving fields are applied simultaneously or sequentially. Assuming the system responds isotropically to the applied field, the change in entropy caused by the isothermal change in the two fields can be expressed as^[15,17,36,37]

$$\begin{aligned} & \Delta S[T, (0, 0) \rightarrow (x_1, x_2)] \\ &= \Delta S[T, (0, 0) \rightarrow (x_1, 0)] + \Delta S[T, (x_1, 0) \rightarrow (x_1, x_2)]. \quad (3) \end{aligned}$$

The first term on the right is only a single field-induced entropy change that quantifies the caloric effect related to the ferroic property X_1

$$\Delta S[T, (0, 0) \rightarrow (x_1, 0)] = \int_0^{x_1} \left(\frac{\partial X_1}{\partial T} \right)_{x_1, x_2=0} dx_1, \quad (4)$$

while the second term on the right is the caloric effect due to the application of field x_2 at constant x_1 , and it can be written as the sum of terms of the single caloric effect associated

with the induced change of the property X_2 and a caloric cross-response contribution

$$\begin{aligned} & \Delta S[T, (x_1, 0) \rightarrow (x_1, x_2)] \\ &= \Delta S[T, (0, 0) \rightarrow (0, x_2)] \\ &+ \int_0^{x_1} \frac{\partial}{\partial x_1'} [\Delta S[T, (x_1', 0) \rightarrow (x_1', x_2)]] dx_1' \\ &= \int_0^{x_2} \left(\frac{\partial X_2}{\partial T} \right)_{x_1=0, x_2} dx_2 + \int_0^{x_1} \int_0^{x_2} \frac{\partial \chi_{12}}{\partial T} dx_2 dx_1, \quad (5) \end{aligned}$$

where $\chi_{12} = (\partial X_1 / \partial x_2)_{T, x_1} = (\partial X_2 / \partial x_1)_{T, x_2}$ is the cross-susceptibility that quantifies the response of X_1 (X_2) to the nonconjugated field x_2 (x_1). It indicates the strength of the interaction between ferroic properties X_1 and X_2 . Therefore, due to the interaction between ferroic properties X_1 and X_2 , the multicaloric effect is not a simple sum of the caloric effects associated with each one alone. The isothermal entropy change of the multicaloric effect can be written as

$$\begin{aligned} & \Delta S[T, (0, 0) \rightarrow (x_1, x_2)] \\ &= \int_0^{x_1} \left(\frac{\partial X_1}{\partial T} \right)_{x_1, x_2=0} dx_1 + \int_0^{x_2} \left(\frac{\partial X_2}{\partial T} \right)_{x_1=0, x_2} dx_2 \\ &+ \int_0^{x_1} \int_0^{x_2} \frac{\partial \chi_{12}}{\partial T} dx_2 dx_1, \quad (6) \end{aligned}$$

where the last coupled term produces the coupled-caloric effect.

Another useful method for proving the interdependence of thermal response on different external fields is to analyze the caloric effects caused by changes in the ferroic property X_i on the application or removal of the non-conjugated field x_j , and maintain the remaining fields constant. The ferroic property can be expressed as $X_i = X_i(T, x_1, x_2)$, where $i = 1, 2$. One may then express the entropy change by the appropriate Maxwell relations as follows:^[15,17,36,37]

$$\begin{aligned} & \Delta S[T, x_1 = 0, X_1(0) \rightarrow X_1(x_2)] \\ &= - \int_{X_1(0)}^{X_1(x_2)} \left(\frac{\partial x_1}{\partial T} \right)_{x_1, x_2} dX_1, \quad (7) \end{aligned}$$

where $X_1(0)$ and $X_1(x_2)$ are the values of the X_1 variable at $x_2 = 0$ and at a given value of the field x_2 , respectively. Taking into account that

$$\left(\frac{\partial x_1}{\partial T} \right)_{x_1} = - \left(\frac{\partial x_1}{\partial X_1} \right)_T \left(\frac{\partial X_1}{\partial T} \right)_{x_1}, \quad (8)$$

and $dX_1 = \left(\frac{\partial X_1}{\partial x_2} \right) dx_2$, from Eqs. (6)–(8), the entropy change $\Delta S[T, x_1 = 0, X_1(0) \rightarrow X_1(x_2)]$ can be expressed as

$$\begin{aligned} & \Delta S[T, x_1 = 0, X_1(0) \rightarrow X_1(x_2)] \\ &= \int_0^{x_2} \frac{\left(\frac{\partial X_1}{\partial x_2} \right)}{\left(\frac{\partial x_1}{\partial X_1} \right)_T} \left(\frac{\partial X_1}{\partial T} \right)_{x_1=0, x_2} dx_2. \quad (9) \end{aligned}$$

3. Theoretical approaches

3.1. First-principles calculations

First-principles calculation plays a very fruitful role in the theoretical understanding of the multicaloric effect. Lisenkov *et al.* used first-principles simulations to study the multicaloric effect in a typical ferroelastic/ferroelectric PbTiO_3 , providing insights into the multicaloric effect of the material.^[16] To explore the multicaloric nature of PbTiO_3 , they used the direct approach^[66,67] to calculate the caloric change directly. The total energy of PbTiO_3 is given by the effective Hamiltonian by the first-principles calculation. This Hamiltonian correctly predicts various structural and thermodynamic properties of PbTiO_3 , including polarization, Curie temperature, and some others. In addition, the total energy given by the Hamiltonian was used in the framework of an isenthalpic Monte Carlo simulation, which simulates the electrocaloric effect induced by a single electric field, the barocaloric effect induced by a single stress field, and the multicaloric effect induced by the electric field and pressure simultaneously. Their work found that the multicaloric effect far exceeds either piezocaloric or electrocaloric effect in the same material. In addition, when multiple external fields are applied, the strong coupling between the two ferroic order parameters plays a key role in the significant enhancement of the caloric effect. This study clearly shows that first-principles calculations are of great significance for understanding the multicaloric effect from a theoretical perspective.

3.2. Landau theory

The Landau model can also be used to describe the multiple thermal properties near phase transitions in the system. This model combines the coupling between the ordered parameters related to two ferroic properties. Planes *et al.* discussed the multicaloric effect under the combined action of a magnetic field and an electric field based on a system with a magnetoelectric coupling.^[37,68] The related order parameters are the magnetization M and the polarization P . Therefore, the proposed Landau free energy contains pure terms related to the polar and magnetic contributions and terms that explain their interaction. That is, the free energy can be expressed as

$$F = F_P(T, P) + F_M(T, M) + F_{P-M}(P, M). \quad (10)$$

In the Landau phase transition theory, the following free energy contributions can be obtained:

$$F_P(T, P) = F_P(T) + \frac{1}{2}aP^2 + \frac{1}{4}bP^4 + \frac{1}{6}cP^6 + \dots, \quad (11)$$

$$F_M(T, M) = F_M(T) + \frac{1}{2}\alpha M^2 + \frac{1}{4}\beta M^4 + \frac{1}{6}\gamma M^6 + \dots, \quad (12)$$

$$F_{P-M}(P, M) = \frac{1}{2}\kappa P^2 M^2, \quad (13)$$

where κ represents the magnetoelectric coefficient. Furthermore, according to the Curie–Weiss law,

$$a = \chi_P^{-1} = \eta_P(T - T_c^P), \quad (14)$$

$$\alpha = \chi_M^{-1} = \eta_M(T - T_c^M), \quad (15)$$

where T_c^P and T_c^M are the paraelectric transition temperature and paramagnetic Curie temperature, respectively.

They assumed $b > 0$, $\beta > 0$, and $\gamma > 0$ to ensure that the pure ferroelectric and ferromagnetic free energy functions are positive definitely for large values of P and M . Electric field E and magnetic field H can be introduced by introducing Gibbs-like polar and magnetic free energies

$$G_P = F_P - EP, \quad (16)$$

$$G_M = F_M - HM. \quad (17)$$

The minimum of the Gibbs free energy $G = G_P + G_M + F_{P-M}$ relative to P gives the relationship between P and M ,

$$bP^3 + aP + \kappa PM^2 = E. \quad (18)$$

When the applied electric field is zero, the following relationship exists in the ferroelectric phase:

$$P^2 = -(a + \kappa M^2)/b. \quad (19)$$

Therefore, the effective magnetic Gibbs free energy can be expressed as

$$G_{\text{eff}} = G_0(T) + \frac{1}{2}A(T, \kappa)M^2 + \frac{1}{4}B(\kappa)M^4 + \frac{1}{6}\gamma M^6 - HM,$$

with

$$G_0(T) = -\frac{a(T)^2}{4b}, \quad A(T, \kappa) = \alpha(T) - \kappa \frac{a(T)}{b},$$

$$B(\kappa) = \beta - \frac{\kappa^2}{b}. \quad (20)$$

From the Landau phase transition theory, the sign of the fourth-order coefficient $B(\kappa)$ predicts that the magnetoelectric phase transition might be continuous or discontinuous. According to the above model, Plane *et al.* established a phase diagram of the magnetoelectric coupling coefficient and temperature, and pointed out that the slope of the coexistence line in the E – H diagram at a given temperature can be given by the generalized Clausius–Clapeyron equation in a first-order phase transition material

$$\frac{dE}{dH} = -\frac{\Delta M}{\Delta P}. \quad (21)$$

The pure electrocaloric effect can be obtained by the following equation:

$$S(T, 0 \rightarrow E)$$

$$= -\frac{\partial G_P}{\partial T} = S_0(T) - \frac{1}{2}\eta_P P^2(T, E)$$

$$= -\frac{1}{2}\eta_P [P^2(T, E) - P^2(T, 0)] = \int_0^E \left(\frac{\partial P}{\partial T} \right)_E dE, \quad (22)$$

where $S_0(T) = a(T)/(2b)$ and $P^2(T, E)$ is a solution of $\partial G_P/\partial P = 0$. In addition, at constant temperature, $(\partial P/\partial T)_E dE = -\eta_P P dP$.

Furthermore, the isothermal entropy change induced by the magnetic field H can be expressed as the sum of the polar and magnetic contributions

$$\Delta S(T, E = 0, 0 \rightarrow H) = \Delta S_P[T, E = 0, P(0) \rightarrow P(H)]$$

$$+ \Delta S_M[T, E = 0, M(0) \rightarrow M(H)], \quad (23)$$

where the cross-caloric term associated with the polar induced by the magnetic field is given by

$$\Delta S_P[T, E = 0, P(0) \rightarrow P(H)] = S_P(T, H) - S_0(T, 0)$$

$$= \frac{1}{2}\eta_P \frac{\kappa}{b} [M^2(T, H) - M^2(T, 0)], \quad (24)$$

and the pure magnetic contribution is given by

$$\Delta S_M[T, E = 0, M(0) \rightarrow M(H)] = S_M(T, H) - S_M(T, 0)$$

$$= -\frac{1}{2}\eta_M [M^2(T, H) - M^2(T, 0)]. \quad (25)$$

Therefore, the isothermal entropy change of the multicaloric effect induced by the simultaneous application of magnetic and electric fields can be obtained as

$$\Delta S(T, 0 \rightarrow E, 0 \rightarrow H)$$

$$= \Delta S(T, E = 0, 0 \rightarrow H) + \Delta S(T, 0 \rightarrow E, H), \quad (26)$$

where

$$\Delta S(T, 0 \rightarrow E, H)$$

$$= -\frac{\partial}{\partial T} \{G_{\text{eff}}[T, M(H, E)] - G_{\text{eff}}[T, M(H, 0)]\},$$

in this case, the relationship between P and M can be given by Eq. (19), and $M(H, E)$ is the solution of $\partial G_{\text{eff}}/\partial M = \partial F_{\text{eff}}/\partial M - H = 0$.

Plane *et al.* used these expressions to investigate the multicaloric effect within Landau theory.^[36,37] The authors found that the application of both magnetic and electric fields can improve the whole effect when both the magnetic and polar contributions are conventional. In other words, when the signs of the entropy change of caloric effect induced by the magnetic field and the electric field are opposite, the magnitude of the multicaloric effect will be lower than that of the caloric effect induced by a certain single field.^[36] They also analyzed the multicaloric effect in the magnetostructural metamagnetic shape-memory materials with a Landau model. Their phenomenological Landau results combined with first-principle calculations provide a route for designing materials with improved multicaloric effects.^[37] Furthermore, several authors have studied the ferroelastic/ferroelectric single

crystals within this framework.^[35,69] Liu *et al.* reported the multicaloric effect in BaTiO₃ single crystals driven simultaneously by mechanical and electric fields, which was described via the Landau free-energy model. They found that the multicaloric behavior is mainly dominated by the mechanical field rather than the electric field, since the paraelectric-to-ferroelectric transition is more sensitive to the mechanical field than to the electric field.^[35] Meng *et al.* used a phenomenological calculation based on the Landau phase transition theory to evaluate the magnitude of the coupled-caloric effect in a ferromagnetic–ferroelectric system. Their results indicated that the magneto-electric coupling greatly strengthens the magnetization, ferroelectric polarization, and isothermal entropy change in the coupled ferromagnetic-ferroelectric multiferroic system. The caloric effect in the coupled system is greatly enhanced by increasing the magneto-electric coupling strength.^[69]

3.3. Mean field model

To describe the multicaloric effect of specific materials in more detail, a reliable approach is to consider the mean field model which captures the internal mechanism expected to be more important. Stern-Taulats *et al.* used the mean field model for the free energy of the FeRh bulk to describe the antiferromagnetic (AFM) to ferromagnetic (FM) phase transition.^[17] The model includes a magnetovolumic coupling term to account for the changes in unit cell volume during transition, and the coupling term includes the effect of external fields such as pressure P and magnetic field H . The total free energy of the system is $f = f_{\text{mag}} + f_{\text{coupling}}$, and the variational Gibbs energy function per magnetic atom is

$$\begin{aligned}
 g^* = & \frac{g}{zJ_{\text{FeRh}}^{(1)}} = -\frac{1}{2}m_{\text{Fe}}m_{\text{Rh}} - \frac{J^*}{4}(m_{\text{Fe}}^2 - \eta_{\text{Fe}}^2) \\
 & + \frac{T^*}{8}[(1 + m_{\text{Fe}} + \eta_{\text{Fe}})\ln(1 + m_{\text{Fe}} + \eta_{\text{Fe}}) \\
 & + (1 - m_{\text{Fe}} - \eta_{\text{Fe}})\ln(1 - m_{\text{Fe}} - \eta_{\text{Fe}}) \\
 & + (1 + m_{\text{Fe}} - \eta_{\text{Fe}})\ln(1 + m_{\text{Fe}} - \eta_{\text{Fe}}) \\
 & + (1 - m_{\text{Fe}} + \eta_{\text{Fe}})\ln(1 - m_{\text{Fe}} + \eta_{\text{Fe}}) \\
 & + 2(1 + m_{\text{Rh}})\ln(1 + m_{\text{Rh}}) \\
 & + 2(1 - m_{\text{Rh}})\ln(1 - m_{\text{Rh}}) - 8\ln 2] \\
 & + \frac{1}{2}\alpha_0^*\omega^2 - \alpha_1^*\omega(m_{\text{Fe}} + m_{\text{Rh}})^2 \\
 & - \alpha_2^*\omega\eta_{\text{Fe}}^2 - H^*(m_{\text{Fe}} + m_{\text{Rh}}) + P\Omega_0^*\omega, \quad (27)
 \end{aligned}$$

where m_{Fe} and m_{Rh} are the order parameters that describe the ferromagnetism of the sublattices of Fe and Rh; η_{Fe} is the AFM order parameter of Fe; ω is the relative volume change; α_1 and α_2 are the magnetostriction coefficients, and α_0 is the inverse of the compressibility. J is an effective exchange interaction parameter and z refers to the coordination number of the first neighbors.

Therefore, the entropy S of the system can be directly computed from Eq. (27) by employing the thermodynamic definition of S ,

$$\begin{aligned}
 S(m_{\text{Fe}}, m_{\text{Rh}}, \eta_{\text{Fe}}) \\
 = -[\partial g^*/\partial T^*]_{P,H} = S_{\text{Fe}}(m_{\text{Fe}}, \eta_{\text{Fe}}) + S_{\text{Rh}}(m_{\text{Rh}}), \quad (28)
 \end{aligned}$$

where $m_{\text{Fe}}(T, H, P)$, $m_{\text{Rh}}(T, H, P)$, and $\eta_{\text{Fe}}(T, H, P)$ are the equilibrium order parameters. The isothermal entropy change for the multicaloric effect induced by the application of pressure and magnetic field can be calculated from

$$\Delta S(T, 0 \rightarrow H, 0 \rightarrow P) = S(T, H, P) - S(T, H = 0, P = 0).$$

Stern-Taulats *et al.* also studied the multicaloric effect and the effects of hysteresis within this mean field approximation and the model also nicely reproduced the experimental data of the magnetostructural coupled system (bulk FeRh) over a broad range of pressure, magnetic field, and temperature.^[17]

4. Experiment approaches

Previous theoretical studies have shown that the huge thermal response of a multiferroic material to an applied magnetic/electric field or stress originates from the strong coupling interaction between spin/polar and lattice. Due to the cross-response to mechanical, magnetic or electric fields, it is expected that the multicaloric effect driven by multiple fields can enhance the caloric effect and overcome some shortcomings such as the limitation of the cooling temperature window and irreversibilities due to hysteresis. However, most of previous experimental studies focused on the effect of hydrostatic pressure on the magnetocaloric effect and the electrocaloric effect. Hydrostatic pressure, as a clean means compared to chemical pressure, has been successfully used to tune the temperature position through impacting the magnetostructural/magnetoelastic transition for the giant MCE materials. However, the magnitude of MCE could be seldom enhanced by a physical pressure except for a few cases where the enhanced MCE mainly originates from the enhanced contribution of the lattice and the strengthening of the first-order transition by the pressure.^[11–13] For example, the application of hydrostatic pressure on Tb₅Si₂Ge₂ compound^[11] can significantly enhance the MCE by changing the phase transition from second-order to first-order in nature. Large enhancements of magnetocaloric and barocaloric effects by hydrostatic pressure were also observed in La(Fe_{0.92}Co_{0.08})_{11.9}Si_{1.1} compound,^[12] which mainly originate from the increased contribution of the lattice entropy change (ΔS_{Latt}). Neutron powder diffraction revealed that the hydrostatic pressure sharpens the magnetoelastic transition and enlarges the volume change, $\Delta V/V$, during the magnetoelastic transition through altering the specific atomic environments of NaZn₁₃-type structure.^[12] For

the Ni₂In-type hexagonal (MnNiSi)_{1-x}(MnFeGe)_x alloys, enhanced MCE by hydrostatic pressure was also observed, which was ascribed to the enlarged $\Delta V/V$ across the magnetostructural transition.^[13] The estimated enhancement of $\Delta V/V$ is up to 7% by pressure according to the relation between the ΔS_{Latt} and volume change $\Delta V/V$, i.e., $\delta[\Delta V/V(\%)]/\delta(\Delta S_{\text{Latt}}) = 0.08 \text{ J}\cdot\text{kg}^{-1}\cdot\text{K}^{-1}$.

Moreover, for the MCE materials with magnetostructural/magnetoelastic transition, the inherent hysteresis loss can be reduced through dual-field regulation or multicaloric cycle. For example, a reduction of magnetic hysteresis has been observed in Ni–Mn–In–Co bulk, where the sample is magnetized at ambient pressure while demagnetized under 1.3 kbar.^[29] FeRh alloys have also been studied from this perspective. Liu *et al.* reduced the magnetic hysteresis loss by 96% in a dual-field magnetic-electric refrigeration cycle for FeRh/BaTiO₃ heterostructures.^[30] The multicaloric cycle gives rise to larger reversible caloric effect than any single field. The same situation was demonstrated in the multicaloric cycle of FeRh/PMN-PT heterostructure.^[32] Qiao *et al.* reported a nonvolatile reduction of hysteresis loss in FeRh film, and quantitative analysis indicated that the effective refrigeration capacity (RC_{eff}) can be increased to a new height by utilizing the external mechanical work as long as the nonvolatile strain can be large enough.

The findings discussed above provide important guidance for significantly enhancing the caloric effects and reducing the hysteresis loss through multi-field regulation. However, in these studies, the applied stress usually kept constant and the coupling term driven by the combined application of magnetic field and pressure was not taken into account. The main obstacle lies in the fact that it is difficult to realize a continuously changing stress field in reality. So far, only two experimental studies of multicaloric effect have considered the cou-

pling terms, where the function of magnetization as pressure was obtained by a nonlinear numerical simulation based on the magnetization data collected under different pressures. One is the Fe₄₉Rh₅₁^[17] and the other is the Ni₅₀Mn₃₅In₁₅ alloys.^[15] However, it is worth noting that the pressure and magnetic fields have opposite effects on the magnetostructural transition for these two alloys. Currently, almost no study has been conducted on systems in which the magnetic field and hydrostatic pressure drive the phase transition in the same direction.

4.1. FeRh alloys

FeRh alloys have attracted considerable attention in recent years due to their large magnetocaloric,^[70] elastocaloric,^[71] and barocaloric^[72] effects. FeRh is an ideal material for studying the fundamentals of multicaloric effect, which undergoes a magnetoelastic transition from a low temperature AFM to a high temperature FM phase. The crystal structure remains the CsCl-type cubic (*Pm3m*) but the lattice expands isotropically by $\Delta V/V \sim 1\%$ on heating during the transition for Fe₄₉Rh₅₁ alloys.^[17,72] Therefore, the application of magnetic field and hydrostatic pressure has opposite effect on the magnetoelastic transition. The former drives the transition to low temperature while the latter drives the transition to high temperature (Fig. 1(a)). In other words, Fe₄₉Rh₅₁ exhibits inverse magnetocaloric effect and conventional barocaloric effect. A proper combination of pressure and magnetic field can not only achieve a significant broadening of the cooling temperature zone, but also reverse the sign of the entropy change from conventional to inverse. In 2015, Stern-Taulats *et al.*^[17] performed magnetic measurements under different hydrostatic pressures, and then the relationship between the magnetization and the pressure (M – P curve) at a specific temperature was obtained by a nonlinear numerical simulation (Fig. 1(b)).

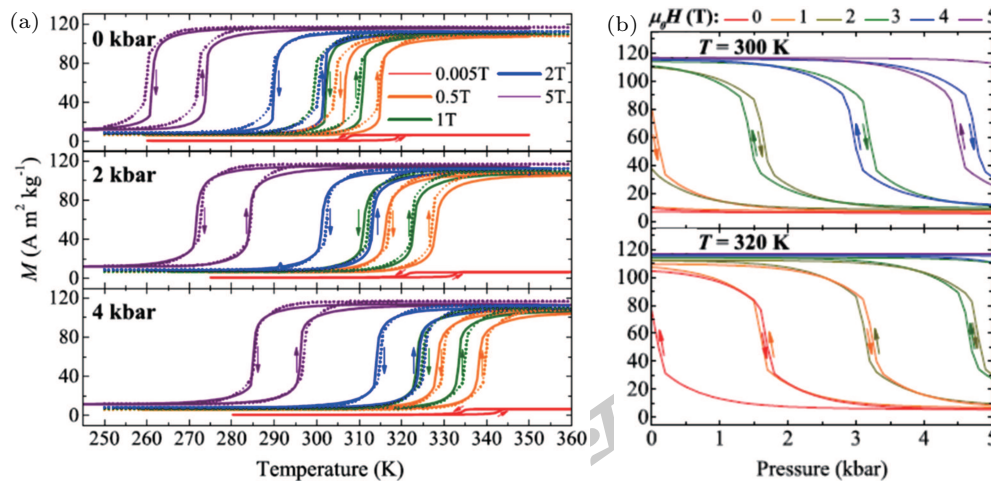


Fig. 1. (a) Thermomagnetic curves of Fe₄₉Rh₅₁ alloy under different magnetic fields and pressures. (b) Isothermal magnetization as a function of pressure for Fe₄₉Rh₅₁ at 300 K and 320 K. (Reprinted with permission from Ref. [17]. Copyright 2017, APS Publishing Limited).

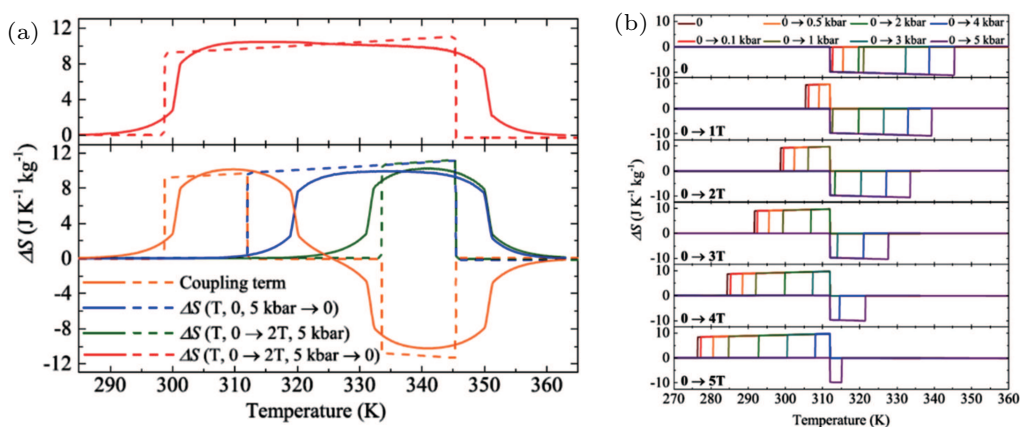


Fig. 2. (a) Temperature dependence of the multicaloric effect (red line), single barocaloric effect under zero magnetic field (blue line), single magnetocaloric effect at 5 kbar (green line), and the coupled-caloric effect (orange line) in $\text{Fe}_{49}\text{Rh}_{51}$ corresponding to the application of a 2 T magnetic field and the removal of 5 kbar pressure. (b) Temperature dependence of the multicaloric effect for combined application of magnetic field and hydrostatic pressure. (Reprinted with permission from Ref. [17]. Copyright 2017, APS Publishing Limited).

By using the thermodynamic relationship in Section 2, quantitative data of the entropy changes of the coupled-caloric and multicaloric effects were obtained based on the M - P curves. Figure 2 shows the temperature dependent entropy changes of multicaloric, single magnetocaloric, single barocaloric, and coupled-caloric effects under the combined application of hydrostatic pressure and magnetic field. It can be observed that, for the thermodynamic path where the magnetic field is applied and the pressure is removed, the single magnetocaloric (Fig. 2(a), green line) and the single barocaloric (Fig. 2(a), blue line) effects are both limited to a narrow temperature range. While the multicaloric effect (Fig. 2(a), red line) shows a significantly broadened cooling temperature region, which is contributed by the cross-response, i.e., the so called coupled-caloric effect (Fig. 2(a), orange line). However, for the thermodynamic path where the magnetic field and pressure are both applied at the same direction, the combination of the inverse magnetocaloric effect and the conventional barocaloric effect will produce a special multicaloric response in $\text{Fe}_{49}\text{Rh}_{51}$, as shown in Fig. 2(b). At lower magnetic fields, the conventional barocaloric effect plays a dominant role, and the application of pressure reduces the total entropy change. As the magnetic field increases, the effect of the inverse magnetocaloric effect gradually increases. When the magnetic field increases to a certain value, the sign of the multicaloric effect in $\text{Fe}_{49}\text{Rh}_{51}$ alloy changes from negative to positive, and the cooling temperature region shifts to lower temperature. It proves that, due to the different performance of the coupled-caloric effect, the sign of the multicaloric response can be finely adjusted by application of magnetic field and hydrostatic pressure. These performances of the thermodynamic path dependence of the multicaloric effect are closely related to the opposite effects of magnetic field and pressure on the phase transition. However, the physical mechanism of the coupled-caloric effect is not involved in this work, which requires further research.

4.2. Ni-Mn-based Heusler alloys

In order to further study the physical mechanism behind the coupled-caloric effect, Liang *et al.* investigated the coupled-caloric effect driven by combined hydrostatic pressure and magnetic field in $\text{Ni}_{50}\text{Mn}_{35}\text{In}_{15}$ alloy by using the measured magnetization data under different pressures.^[15] It is worth noting that the driving direction of pressure for the martensitic magnetostructural transition of the off-stoichiometric Heusler alloy $\text{Ni}_2\text{Mn}_{1+x}\text{In}_{1-x}$ is also opposite to that of the magnetic field. The off-stoichiometric Heusler alloy $\text{Ni}_2\text{Mn}_{1+x}\text{M}_{1-x}$ ($M = \text{Ga}, \text{Sn}$ and In , $0 < x < 1$) undergoes a martensitic transformation from a high temperature $L2_1$ cubic structure to a closely packed martensite phase with low crystal symmetry.^[73] Many important functional properties related to the martensitic transition have been reported, such as metamagnetic shape memory effect,^[74] magnetic superelasticity,^[75] giant magnetocaloric effect, and magnetoresistance.^[76] The application of hydrostatic pressure compresses the lattice and shortens the nearest neighboring atomic distance of Mn-Mn. As a response, the AFM exchange between the Mn atoms enhances, resulting in the shift of the martensitic transition temperature (T_M) to higher temperature.^[77] Meanwhile, the alloys exhibit a big difference of magnetization between the FM austenitic and non-magnetic/PM martensitic phases near the transition temperature. The resultant large difference of Zeeman energy ensures that the martensitic transition can be driven to lower temperature by an external magnetic field.^[78] Therefore, the off-stoichiometric $\text{Ni}_2\text{Mn}_{1+x}\text{In}_{1-x}$ is also an ideal platform for investigating the fundamentals of multicaloric effect driven by magnetic field and pressure. Studies indicated that,^[15] in the temperature region of phase transition for $\text{Ni}_{50}\text{Mn}_{35}\text{In}_{15}$ alloy, the effect of pressure on magnetic properties can be expressed by the change of magnetic volume coupling coefficient χ_{12} caused by pressure. The macroscopic physical meaning of χ_{12} refers to the change of magnetism driven by the external pressure at a certain temperature

in the phase transition region. By measuring the thermomagnetic curves under different magnetic fields and pressures, the relationship between magnetization and pressure at a specific temperature (M - P curve) can be obtained by nonlinear fitting. Then, the magnetic volume coupling coefficient χ_{12} is derived from the M - P curves by the equation $\chi_{12} = (\partial M / \partial P)_{T, \mu_0 H}$. Figure 3 shows the colored contour map and two-dimensional (2D) plots of magnetic volume coupling coefficient χ_{12} as functions of pressure and temperature under 5 T magnetic field. With the increase of pressure, the peak position of χ_{12} gradually moves to higher temperature, and the peak always appears near T_M regardless of the pressure. It is worth noting that, according to Eq. (5), the coupled-caloric effect is the double integral of the magnetic volume coupling coefficient χ_{12} ($\Delta S_{cp} = \int_0^P \int_0^H \partial \chi_{12} / \partial T dH dP$), so the evolution of χ_{12} with pressure and temperature directly reflects the characteristic behavior of the coupling caloric effect.

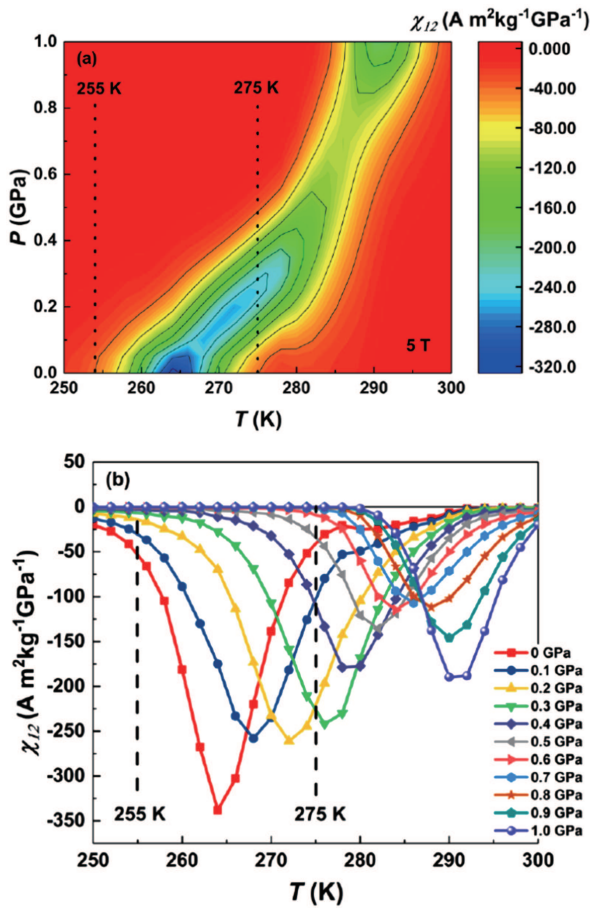


Fig. 3. (a) Colored contour map and (b) two-dimensional plots of magnetic volume coupling coefficient χ_{12} as functions of pressure and temperature. (Reprinted with permission from Ref. [15]; licensed under a Creative Commons Attribution (CC BY) license).

The coupled-caloric effects and magnetocaloric effects under certain pressure have been calculated based on the M - P and M - H curves using thermodynamic formulas in Section 2. The application of different pressures and the removal of magnetic field from 5 T to 0 were chosen as the thermodynamic

path. For the entropy change of the coupled-caloric effect (Figs. 4(a) and 4(b)), a negative peak gradually increases in width and depth with increasing pressure near a low temperature of 264 K, while a positive peak forms in the high temperature region (Figs. 4(a) and 4(b)). In other words, the entropy change of the coupled-caloric effect shows a separation of positive and negative peaks. Comparison of the entropy change of the calculated and experimentally measured magnetocaloric effects indicates the caloric effect driven by magnetic field under a certain pressure is the magnetocaloric effect at ambient pressure adjusted by the coupled-caloric effect (Fig. 4(c)). The negative peak of the coupled-caloric effect in the low temperature range compensates the entropy change at ambient

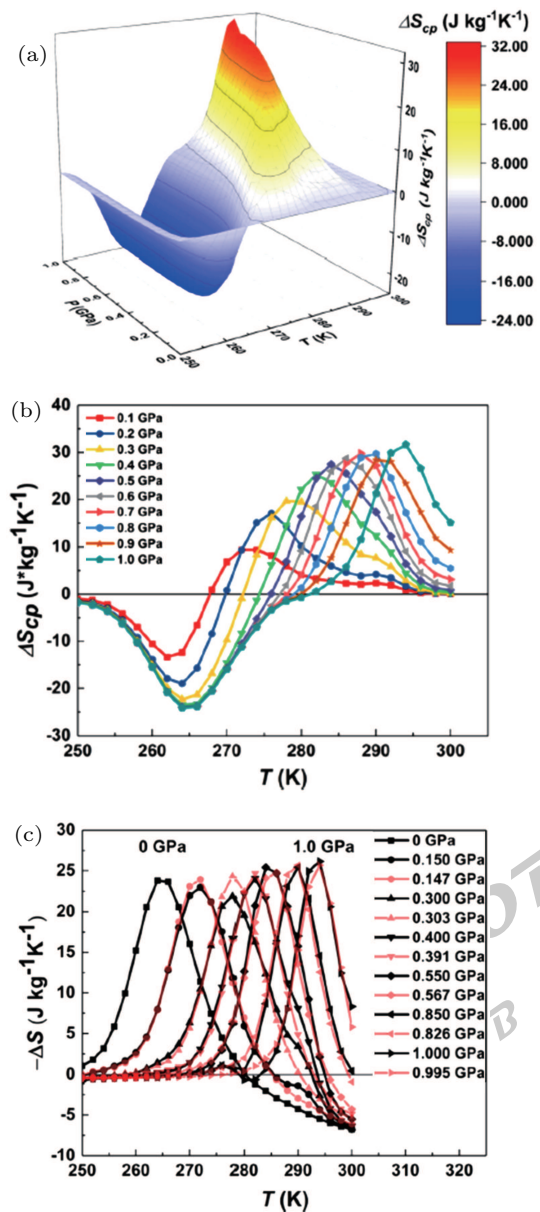


Fig. 4. (a) The 3D and (b) 2D plots of the coupled-caloric effect as a function of pressure and temperature for a magnetic field change of 5–0 T. (c) Comparison of the entropy change at ambient pressure adjusted by the coupled-caloric effect and the magnetocaloric results at a specific pressure calculated using Maxwell relation. (Reprinted with permission from Ref. [15]; licensed under a Creative Commons Attribution (CC BY) license).

pressure. While the positive peak of the coupled-caloric effect, which reflects the evolution of magnetic-structural coupling with pressure, contributes to the entropy change at high pressure. Although the pressure of 9.95 kbar reduces the change in magnetization (ΔM) across the T_M by 20%, the contribution of the coupled-caloric effect makes the magnetic entropy change enhanced by 8%. Via quantitatively analyzing the coupled-caloric effect, the essence of the regulated magnetocaloric effect by pressure is revealed in this work, which is of significance for designing new materials based on the magnetostructural coupling strength and its sensitivity to pressure.

5. Outlook

For the material with first-order transition, the multicaloric effect driven by multiple fields can overcome some inherent limitations of single caloric effect by improving its thermal response and reversibility. Quantitative analysis about the coupling term contributed to the multicaloric effect can promote the understanding of the refrigeration process controlled by multiple fields. Through pioneer efforts, the multicaloric effect can be understood theoretically in enough detail. However, due to the limitations of experimental technology, few experimental studies have focused on the coupled-caloric and multicaloric effects. The main obstacle lies in the fact that it is difficult to realize a continuously changing stress field in reality. So far, only two experimental studies of multicaloric effect have considered the coupling terms, where the function of magnetization as pressure was obtained by a non-linear numerical simulation based on the magnetization data collected under different pressures. One is the $\text{Fe}_{49}\text{Rh}_{51}$ and the other is the $\text{Ni}_{50}\text{Mn}_{35}\text{In}_{15}$ alloys. Although the driving directions of magnetostructural/magnetoelastic transition by magnetic field and hydrostatic pressure are opposite for both alloys, a proper choice of the thermodynamic path can lead to an enhanced and broadened caloric response.

The entropy change of the coupled-caloric effect shows separated positive and negative peaks, and the sign of these two peaks depends on the thermodynamic path of the applied pressure and magnetic field. For the materials with opposite driving directions by magnetic field and hydrostatic pressure, the temperature span of the multicaloric effect can be significantly widened in a thermodynamic path where the magnetic field is applied and the pressure is removed; while, the sign of the multicaloric effect is turned over from negative to positive in the thermodynamic path where the magnetic field and pressure are both applied at the same time. In addition, the expression of the coupled-caloric effect is also critically dependent on the strengthening of the first-order transition nature impacted by pressure. Since the materials with the same driving directions by dual fields are very few, there is no experimental report on the coupled-caloric and multicaloric effects

for such systems up to now. However, based on the obtained insights, it can be predicted that the multi-field driving cooling temperature zone will broaden in the same direction if the driving directions of the dual fields are the same. At the same time, the enhancement of the coupled-caloric effect will also innovatively contribute to the multicaloric effect. A combination of the experimental and theoretical methods mentioned above is suggested to be used to systematically study different materials. Such research not only helps to make breakthrough progress in multicaloric cycle refrigeration, but also provides valuable feedback for material developments.

References

- [1] Gschneidner Jr K A, Pecharsky V K and Tsokol A O 2005 *Rep. Prog. Phys.* **68** 1479
- [2] Franco V, Blázquez J S, Ipus J J, Law J Y, Moreno-Ramírez L M and Conde A 2018 *Prog. Mater. Sci.* **93** 112
- [3] Shen B G, Sun J R, Hu F X, Zhang H W and Cheng Z H 2009 *Adv. Mater.* **21** 4545
- [4] Li L W and Yan M 2020 *J. Alloys Compd.* **823** 153810
- [5] Zheng X Q and Shen B G 2017 *Chin. Phys. B* **26** 027501
- [6] Li Z X, Li K, Shen J, Dai W, Gao X Q, Guo X H and Gong M Q 2017 *Acta Phys. Sin.* **66** 110701 (in Chinese)
- [7] Neese B, Chu B, Lu S G, Wang Y, Furman E and Zhang Q M 2008 *Science* **321** 821
- [8] Manosa L and Planes A 2017 *Adv. Mater.* **29** 1603607
- [9] Tušek J, Engelbrecht K, Eriksen D, Dall'Olio S, Tušek J and Pryds N 2016 *Nat. Ener.* **1** 16134
- [10] Moya X, Kar-Narayan S and Mathur N D 2014 *Nat. Mater.* **13** 439
- [11] Morellon L, Arnold Z, Magen C, Ritter C, Prokhnenko O, Skorokhod Y, Algarabel P A, Ibarra M R and Kamarad J 2004 *Phys. Rev. Lett.* **93** 137201
- [12] Hao J Z, Hu F X, Wang J T, Shen F R, Yu Z B, Zhou H B, Wu H, Huang Q Z, Qiao K M, Wang J, He J, He L H, Sun J R and Shen B G 2020 *Chem. Mater.*
- [13] Samanta T, Lepkowski D L, Saleheen A U, Shankar A, Prestigiacomo J, Dubenko I, Quetz A, Oswald I W H, McCandless G T, Chan J Y, Adams P W, Young D P, Ali N and Stadler S 2015 *Phys. Rev. B* **91** 020401
- [14] Chauhan A, Patel S and Vaish R 2015 *Acta Mater.* **97** 17
- [15] Liang F X, Hao J Z, Shen F R, Zhou H B, Wang J, Hu F X, He J, Sun J R and Shen B G 2019 *APL Mater.* **7** 051102
- [16] Lisenkov S, Mani B K, Chang C M, Almand J and Ponomareva I 2013 *Phys. Rev. B* **87** 224101
- [17] Stern-Taulats E, Castán T, Planes A, Lewis L H, Barua R, Pramanick S, Majumdar S and Mañosa L 2017 *Phys. Rev. B* **95** 104424
- [18] Pecharsky V K and Gschneidner Jr. K A 1997 *Phys. Rev. Lett.* **78** 4494
- [19] Hu F X, Shen B G, Sun J R and Zhang X X 2000 *Chin. Phys.* **9** 550
- [20] Fujita A, Fujieda S, Hasegawa Y and Fukamichi K 2003 *Phys. Rev. B* **67** 104416
- [21] Castillo-Villa P O, Soto-Parra D E, Matutes-Aquino J A, Ochoa-Gamboa R A, Planes A, Mañosa L, González-Alonso D, Stipcich M, Romero R, Ríos-Jara D and Flores-Zúñiga H 2011 *Phys. Rev. B* **83** 174109
- [22] Wada H and Tanabe Y 2001 *Appl. Phys. Lett.* **79** 3302
- [23] ul Hassan N, Shah I A, Khan T, Liu J, Gong Y, Miao X and Xu F 2018 *Chin. Phys. B* **27** 037504
- [24] Yang H, Liu J, Li C, Wang G L, Gong Y Y and Xu F 2018 *Chin. Phys. B* **27** 107502
- [25] Bao L F, Huang W D and Ren Y J 2016 *Chin. Phys. Lett.* **33** 077502
- [26] Zhang H, Xing C F, Long K W, Xiao Y N, Tao K, Wang L C and Long Y 2018 *Acta Phys. Sin.* **67** 207501 (in Chinese)
- [27] Zhang B, Zheng X Q, Zhao T Y, Hu F X, Sun J R and Shen B G 2018 *Chin. Phys. B* **27** 067503
- [28] Trung N T, Ou Z Q, Gortemulder T J, Tegus O, Buschow K H J and Brück E 2009 *Appl. Phys. Lett.* **94** 102513
- [29] Liu J, Gottschall T, Skokov K P, Moore J D and Gutfleisch O 2012 *Nat. Mater.* **11** 620

- [30] Liu Y, Phillips L C, Mattana R, Bibes M, Barthelemy A and Dkhil B 2016 *Nat. Commun.* **7** 11614
- [31] Liu J, Gong Y, You Y, You X, Huang B, Miao X, Xu G, Xu F and Brück E 2019 *Acta Mater.* **174** 450
- [32] Qiao K, Hu F, Liu Y, Li J, Kuang H, Zhang H, Liang W, Wang J, Sun J and Shen B 2019 *Nan. Ener.* **59** 285
- [33] Guillou F, Pathak A K, Paudyal D, Mudryk Y, Wilhelm F, Rogalev A and Pecharsky V K 2018 *Nat. Commun.* **9** 2925
- [34] Scheibel F, Gottschall T, Taubel A, Fries M, Skokov K P, Terwey A, Keune W, Ollefs K, Wende H, Farle M, Acet M, Gutfleisch O and Gruner M E 2018 *Ener. Techno* **6** 1397
- [35] Liu Y, Zhang G, Li Q, Bellaiche L, Scott J F, Dkhil B and Wang Q 2016 *Phys. Rev. B* **94** 214113
- [36] Planes A, Castán T and Saxena A 2014 *Philos. Mag.* **94** 1893
- [37] Planes A, Castán T and Saxena A 2016 *Philos. Trans. R. Soc. A* **374** 20150304
- [38] Chauhan A, Patel S and Vaish R 2015 *Acta Mater.* **89** 384
- [39] Li L W 2016 *Chin. Phys. B* **25** 037502
- [40] Zheng X Q, Shen J, Hu F X, Sun J R and Shen B G 2016 *Acta Phys. Sin.* **65** 217502 (in Chinese)
- [41] Zhang Y 2019 *J. Alloys Compd.* **787** 1173
- [42] Hao Z H, Wang H Y, Zhang Q and Mo Z J 2018 *Acta Phys. Sin.* **67** 247502 (in Chinese)
- [43] Wu X F, Guo C P, Cheng G, Li C R, Wang J, Du Y S, Rao G H and Du Z M 2019 *Chin. Phys. B* **28** 057502
- [44] Mo Z J, Sun Q L, Shen J, Yang M, Li Y J, Li L, Liu G D, Tang C C and Meng F B 2018 *Chin. Phys. B* **27** 017501
- [45] De Sousa V, Von Ranke P and Gandra F 2011 *J. Appl. Phys.* **109** 063904
- [46] Li L W, Yuan Y, Xu C, Qi Y and Zhou S Q 2017 *AIP Adv.* **7** 056401
- [47] Wang X, Wang L, Ma Q, Sun G, Zhang Y and Cui J 2017 *J. Alloys Compd.* **694** 613
- [48] Chen J, Zheng X Q, Dong Q Y, Sun J R and Shen B G 2011 *Appl. Phys. Lett.* **99**
- [49] Delyagin N N, Krylov V I and Rozantsev I N 2007 *J. Magn. Magn. Mater.* **308** 74
- [50] Chen J, Zheng X Q, Dong Q Y, Sun J R and Shen B G 2011 *Appl. Phys. Lett.* **99** 122503
- [51] Zheng X Q, Chen J, Xu Z Y, Mo Z J, Hu F X, Sun J R and Shen B G 2014 *J. Appl. Phys.* **115** 17A938
- [52] Ma Y F, Tang B Z, Xia L and Ding D 2016 *Chin. Phys. Lett.* **33** 126101
- [53] Wu C, Ding D and Xia L 2016 *Chin. Phys. Lett.* **33** 016102
- [54] Chen X and Zhao M H 2018 *Acta Phys. Sin.* **67** 197501 (in Chinese)
- [55] Zhang H and Shen B G 2015 *Chin. Phys. B* **24** 127504
- [56] Dong Q, Shen B, Chen J, Shen J, Zhang H and Sun J 2009 *J. Appl. Phys.* **105** 07A305
- [57] Klimczak M and Talik E 2010 *J. Phys.: Conf. Ser.* **200** 092009
- [58] Kaštil J, Javorský P, Kamarad J, Diop L, Isnard O and Arnold Z 2014 *Intermetallics* **54** 15
- [59] Fickenscher T, Rodewald U C, Niepmann D, Mishra R, Eschen M and Pöttgen R 2005 *Z. Naturforsch. B* **60** 271
- [60] Ding D, Zhang Y Q and Xia L 2015 *Chin. Phys. Lett.* **32** 106101
- [61] Dong X, Feng J, Yi Y and Li L 2018 *J. Appl. Phys.* **124** 093901
- [62] Fisher I, Islam Z and Canfield P 1999 *J. Magn. Magn. Mater.* **202** 1
- [63] Hermes W, Rodewald U C and Pöttgen R 2010 *J. Appl. Phys.* **108** 113919
- [64] Li L, Niehaus O, Kersting M and Pöttgen R 2015 *Intermetallics* **62** 17
- [65] Li L, Nishimura K, Kadonaga M, Qian Z and Huo D 2011 *J. Appl. Phys.* **110** 043912
- [66] Lisenkov S and Ponomareva I 2012 *Phys. Rev. B* **86** 104103
- [67] Ponomareva I and Lisenkov S 2012 *Phys. Rev. Lett.* **108** 167604
- [68] Planes A, Stern-Taulats E, Castán T, Vives E, Mañosa L and Saxena A 2015 *Mater. Toda.: Procee* **2** S477
- [69] Meng H, Li B, Ren W and Zhang Z 2013 *Phys. Lett. A* **377** 567
- [70] Nikitin S A, Myalikgulyev G, Tishin A M, Annaorazov M P, Asatryan K A and Tyurin A L 1990 *Phys. Lett. A* **148** 363
- [71] Nikitin S A, Myalikgulyev G, Annaorazov M P, Tyurin A L, Myndyev R W and Akopyan S A 1992 *Phys. Lett. A* **171** 234
- [72] Stern-Taulats E, Planes A, Lloveras P, Barrio M, Tamarit J L, Pramanick S, Majumdar S, Frontera C and Mañosa L 2014 *Phys. Rev. B* **89** 214105
- [73] Kübler J, William A R and Sommers C B 1983 *Phys. Rev. B* **28** 1745
- [74] Kainuma R, Imano Y, Ito W, Sutou Y, Morito H, Okamoto S, Kitakami O, Oikawa K, Fujita A, Kanomata T and Ishida K 2006 *Nature* **439** 957
- [75] Krenke T, Duman E, Acet M, Wassermann E F, Moya X, Manosa L and Planes A 2005 *Nat. Mater.* **4** 450
- [76] Yu S Y, Liu Z H, Liu G D, Chen J L, Cao Z X, Wu G H, Zhang B and Zhang X X 2006 *Appl. Phys. Lett.* **89** 162503
- [77] Sharma V K, Chattopadhyay M K and Roy S B 2011 *J. Phys.: Condens Matter* **23** 366001
- [78] Quetz A, Koshkid'ko Y S, Titov I, Rodionov I, Pandey S, Aryal A, Ibarra-Gaytan P J, Prudnikov V, Granovsky A, Dubenko I, Samanta T, Cwik J, Sánchez Llamazares J L, Stadler S, Lähderanta E and Ali N 2016 *J. Alloys Compd.* **683** 139

JUST FOR AUTHORS
— CHINESE PHYSICS B

Chinese Physics B

Volume 29

Number 4

April 2020

TOPICAL REVIEW — Physics in neuromorphic devices

040703 High-performance synaptic transistors for neuromorphic computing

Hai Zhong, Qin-Chao Sun, Guo Li, Jian-Yu Du, He-Yi Huang, Er-Jia Guo, Meng He, Can Wang, Guo-Zhen Yang, Chen Ge and Kui-Juan Jin

048401 Optoelectronic memristor for neuromorphic computing

Wuhong Xue, Wenjuan Ci, Xiao-Hong Xu and Gang Liu

TOPICAL REVIEW — Magnetism, magnetic materials, and interdisciplinary research

047504 Multicaloric and coupled-caloric effects

Jia-Zheng Hao, Feng-Xia Hu, Zi-Bing Yu, Fei-Ran Shen, Hou-Bo Zhou, Yi-Hong Gao, Kai-Ming Qiao, Jia Li, Cheng Zhang, Wen-Hui Liang, Jing Wang, Jun He, Ji-Rong Sun and Bao-Gen Shen

TOPICAL REVIEW — Advanced calculation & characterization of energy storage materials & devices at multiple scale

048201 Failure analysis with a focus on thermal aspect towards developing safer Na-ion batteries

Yuqi Li, Yaxiang Lu, Liquan Chen and Yong-Sheng Hu

SPECIAL TOPIC — Advanced calculation & characterization of energy storage materials & devices at multiple scale

048202 Comparative calculation on Li^+ solvation in common organic electrolyte solvents for lithium ion batteries

Qi Liu, Feng Wu, Daobin Mu and Borong Wu

048203 Influence of fluoroethylene carbonate on the solid electrolyte interphase of silicon anode for Li-ion batteries: A scanning force spectroscopy study

Jieyun Zheng, Jialiang Liu, Suijun Wang, Fei Luo, Liubin Ben and Hong Li

SPECIAL TOPIC — Ion beam technology

040704 Thermal desorption characteristic of helium ion irradiated nickel-base alloy

Shasha Lv, Rui Zhu, Yumeng Zhao, Mingyang Li, Guojing Wang, Menglin Qiu, Bin Liao, Qingsong Hua, Jianping Cheng and Zhengcao Li

045203 Developing cold-resistant high-adhesive electronic substrate for WIMPs detectors at CDEX

Yuanyuan Liu, Jianping Cheng, Pan Pang, Bin Liao, Bin Wu, Minju Ying, Fengshou Zhang, Lin Chen, Shasha Lv, Yandong Liu and Tianxi Sun

046106 *In situ* luminescence measurement of 6H-SiC at low temperature

Meng-Lin Qiu, Peng Yin, Guang-Fu Wang, Ji-Gao Song, Chang-Wei Luo, Ting-Shun Wang, Guo-Qiang Zhao, Sha-Sha Lv, Feng-Shou Zhang and Bin Liao

(Continued on the Bookbinding Inside Back Cover)

048501 Experimental and computational study of visible light-induced photocatalytic ability of nitrogen ions-implanted TiO₂ nanotubes

Ruijing Zhang, Xiaoli Liu, Xinggang Hou and Bin Liao

SPECIAL TOPIC — Optical field manipulation

040305 Creation of topological vortices using Pancharatnam–Berry phase liquid crystal holographic plates

Xuyue Guo, Jinzhan Zhong, Peng Li, Bingyan Wei, Sheng Liu and Jianlin Zhao

SPECIAL TOPIC — Terahertz physics

047302 Hydrodynamic simulation of chaotic dynamics in InGaAs oscillator in terahertz region

Wei Feng

REVIEW

048101 Overview of finite elements simulation of temperature profile to estimate properties of materials 3D-printed by laser powder-bed fusion

Habimana Jean Willy, Xinwei Li, Yong Hao Tan, Zhe Chen, Mehmet Cagirici, Ramadan Borayek, Tun Seng Heng, Chun Yee Aaron Ong, Chaojiang Li and Jun Ding

RAPID COMMUNICATION

047401 Electronic structure and spatial inhomogeneity of iron-based superconductor FeS

Chengwei Wang, Meixiao Wang, Juan Jiang, Haifeng Yang, Lexian Yang, Wujun Shi, Xiaofang Lai, Sung-Kwan Mo, Alexei Barinov, Binghai Yan, Zhi Liu, Fuqiang Huang, Jinfeng Jia, Zhongkai Liu and Yulin Chen

047502 High pressure synthesis and characterization of the pyrochlore Dy₂Pt₂O₇: A new spin ice material

Qi Cui, Yun-Qi Cai, Xiang Li, Zhi-Ling Dun, Pei-Jie Sun, Jian-Shi Zhou, Hai-Dong Zhou and Jin-Guang Cheng

GENERAL

040201 Nonlocal symmetries and similarity reductions for Korteweg–de Vries–negative-order Korteweg–de Vries equation

Heng-Chun Hu and Fei-Yan Liu

040202 Finite-time Mittag–Leffler synchronization of fractional-order delayed memristive neural networks with parameters uncertainty and discontinuous activation functions

Chong Chen, Zhixia Ding, Sai Li and Liheng Wang

040301 Reconciliation for CV-QKD using globally-coupled LDPC codes

Jin-Jing Shi, Bo-Peng Li and Duan Huang

040302 Generating Kerr nonlinearity with an engineered non-Markovian environment

Fei-Lei Xiong, Wan-Li Yang and Mang Feng

040303 Quantum coherence and correlation dynamics of two-qubit system in spin bath environment

Hao Yang, Li-Guo Qin, Li-Jun Tian and Hong-Yang Ma

- 040304 Efficient scheme for remote preparation of arbitrary n -qubit equatorial states**
Xin-Wei Zha, Min-Rui Wang and Ruo-Xu Jiang
- 040306 Reduction of entropy uncertainty for qutrit system under non-Markov noisy environment**
Xiong Xu and Mao-Fa Fang
- 040501 Lump, lumpoff and predictable rogue wave solutions to a dimensionally reduced Hirota bilinear equation**
Haifeng Wang and Yufeng Zhang
- 040502 Nonlinear continuous bi-inductance electrical line with dissipative elements: Dynamics of the low frequency modulated waves**
S M Ngounou and F B Pelap
- 040503 Novel Woods–Saxon stochastic resonance system for weak signal detection**
Yong-Hui Zhou, Xue-Mei Xu, Lin-Zi Yin, Yi-Peng Ding, Jia-Feng Ding and Ke-Hui Sun
- 040504 Energy cooperation in quantum thermoelectric systems with multiple electric currents**
Yefeng Liu, Jincheng Lu, Rongqian Wang, Chen Wang and Jian-Hua Jiang
- 040701 Preliminary abnormal electrocardiogram segment screening method for Holter data based on long short-term memory networks**
Siying Chen and Hongxing Liu
- 040702 A synthetic optically pumped gradiometer for magnetocardiography measurements**
Shu-Lin Zhang and Ning Cao

ATOMIC AND MOLECULAR PHYSICS

- 043101 Analytical expressions of non-relativistic static multipole polarizabilities for hydrogen-like ions**
Xuesong Mei, Wanping Zhou, Zhenxiang Zhong and Haoxue Qiao
- 043102 Non-Born–Oppenheimer study of the muonic molecule ion $^4\text{He}\mu^+$**
Hang Yang, Meng-Shan Wu, Yi Zhang, Ting-Yun Shi, Kalman Varga and Jun-Yi Zhang
- 043103 Re effects in model Ni-based superalloys investigated with first-principles calculations and atom probe tomography**
Dianwu Wang, Chongyu Wang, Tao Yu and Wenqing Liu
- 043201 Controlling paths of high-order harmonic generation by orthogonal two-color fields**
Ze-Hui Ma, Cai-Ping Zhang, Jun-Lin Ma and Xiang-Yang Miao
- 043202 Controlling electron collision by counterrotating circular two-color laser fields**
Baoqin Li, Xianghe Ren and Jingtao Zhang
- 043203 Coherent 420 nm laser beam generated by four-wave mixing in Rb vapor with a single continuous-wave laser**
Hao Liu, Jin-Peng Yuan, Li-Rong Wang, Lian-Tuan Xiao and Suo-Tang Jia
- 043204 Spin-exchange relaxation of naturally abundant Rb in a K–Rb– ^{21}Ne self-compensated atomic comagnetometer**
Yan Lu, Yueyang Zhai, Yong Zhang, Wenfeng Fan, Li Xing and Wei Quan

043205 Filling gap of combination of gauge and analytical method in KFR-like theory

Jian Li and Feng-Cai Ma

043206 Polarization and fundamental sensitivity of ^{39}K (^{133}Cs)– ^{85}Rb – ^{21}Ne co-magnetometers

Jian-Hua Liu, Dong-Yang Jing, Lin Zhuang, Wei Quan, Jiancheng Fang and Wu-Ming Liu

043701 Two types of highly efficient electrostatic traps for single loading or multi-loading of polar molecules

Bin Wei, Hengjiao Guo, Yabing Ji, Shunyong Hou and Jianping Yin

043702 Influence of driving ways on measurement of relative phase in a two-atoms cavity system

Daqiang Bao, Jingping Xu and Yaping Yang

ELECTROMAGNETISM, OPTICS, ACOUSTICS, HEAT TRANSFER, CLASSICAL MECHANICS, AND FLUID DYNAMICS

044201 Dissipative quantum phase transition in a biased Tavis–Cummings model

Zhen Chen, Yueyin Qiu, Guo-Qiang Zhang and Jian-Qiang You

044501 Conserved quantities and adiabatic invariants of fractional Birkhoffian system of Herglotz type

Juan-Juan Ding and Yi Zhang

044502 Discharge flow of granular particles through an orifice on a horizontal hopper: Effect of the hopper angle

Xin Wang, Hong-Wei Zhu, Qing-Fan Shi and Ning Zheng

PHYSICS OF GASES, PLASMAS, AND ELECTRIC DISCHARGES

045201 Hybrid-PIC/PIC simulations on ion extraction by electric field in laser-induced plasma

Xiao-Yong Lu, Cheng Yuan, Xiao-Zhang Zhang and Zhi-Zhong Zhang

045202 Tunability of Fano resonance in cylindrical core–shell nanorods

Ben-Li Wang

CONDENSED MATTER: STRUCTURAL, MECHANICAL, AND THERMAL PROPERTIES

046101 Fundamental band gap and alignment of two-dimensional semiconductors explored by machine learning

Zhen Zhu, Baojuan Dong, Huaihong Guo, Teng Yang and Zhidong Zhang

046102 Irradiation hardening behaviors of tungsten–potassium alloy studied by accelerated 3-MeV W^{2+} ions

Xiao-Liang Yang, Long-Qing Chen, Wen-Bin Qiu, Yang-Yi-Peng Song, Yi Tang, Xu-Dong Cui, Chang-Song Liu, Yan Jiang, Tao Zhang and Jun Tang

046103 Electrical properties of $\text{Ca}_{3-x}\text{Sm}_x\text{Co}_4\text{O}_{9+\delta}$ ceramics prepared under magnetic field

Xiu-Rong Qu, Yan-Yan Xu, Shu-Chen Lü and Jian-Min Hu

046104 Improved carrier transport in Mn:ZnSe quantum dots sensitized La-doped nano- TiO_2 thin film

Shao Li, Gang Li, Li-Shuang Yang and Kui-Ying Li

- 046105 Nearly golden-ratio order in Ta metallic glass**
Yuan-Qi Jiang and Ping Peng
- 046201 Anisotropic plasticity of nanocrystalline Ti: A molecular dynamics simulation**
Minrong An, Mengjia Su, Qiong Deng, Haiyang Song, Chen Wang and Yu Shang
- 046202 Improvement of high-frequency properties of Co₂FeSi Heusler films by ultrathin Ru underlayer**
Cuiling Wang, Shouheng Zhang, Shandong Li, Honglei Du, Guoxia Zhao and Derang Cao
- 046601 Molecular dynamics simulation of thermal conductivity of silicone rubber**
Wenxue Xu, Yanyan Wu, Yuan Zhu and Xin-Gang Liang
- 046801 Effect of initial crystallization temperature and surface diffusion on formation of GaAs multiple concentric nanoring structures by droplet epitaxy**
Yi Wang, Xiang Guo, Jiemin Wei, Chen Yang, Zijiang Luo, Jihong Wang and Zhao Ding
- 046802 Influence of external load on friction coefficient of Fe–polytetrafluoroethylene**
Xiu-Hong Hao, Deng Pan, Ze-Yang Zhang, Shu-Qiang Wang, Yu-Jin Gao and Da-Peng Gu

CONDENSED MATTER: ELECTRONIC STRUCTURE, ELECTRICAL, MAGNETIC, AND OPTICAL PROPERTIES

- 047101 *Ab initio* study of structural, electronic, thermo-elastic and optical properties of Pt₃Zr intermetallic compound**
Wahiba Metiri and Khaled Cheikh
- 047102 Surface potential-based analytical model for InGaZnO thin-film transistors with independent dual-gates**
Yi-Ni He, Lian-Wen Deng, Ting Qin, Cong-Wei Liao, Heng Luo and Sheng-Xiang Huang
- 047103 *Ab initio* calculations on oxygen vacancy defects in strained amorphous silica**
Bao-Hua Zhou, Fu-Jie Zhang, Xiao Liu, Yu Song and Xu Zuo
- 047104 *In-situ* SiN combined with etch-stop barrier structure for high-frequency AlGaN/GaN HEMT**
Min-Han Mi, Sheng Wu, Ling Yang, Yun-Long He, Bin Hou, Meng Zhang, Li-Xin Guo, Xiao-Hua Ma and Yue Hao
- 047301 Identifying anomalous Floquet edge modes via bulk–edge correspondence**
Huanyu Wang and Wuming Liu
- 047303 Effect of AlGaN interlayer on luminous efficiency and reliability of GaN-based green LEDs on silicon substrate**
Jiao-Xin Guo, Jie Ding, Chun-Lan Mo, Chang-Da Zheng, Shuan Pan and Feng-Yi Jiang
- 047304 Negative bias-induced threshold voltage instability and zener/interface trapping mechanism in GaN-based MIS-HEMTs**
Qing Zhu, Xiao-Hua Ma, Yi-Lin Chen, Bin Hou, Jie-Jie Zhu, Meng Zhang, Mei Wu, Ling Yang and Yue Hao

- 047305 Fabrication and characterization of vertical GaN Schottky barrier diodes with boron-implanted termination**
Wei-Fan Wang, Jian-Feng Wang, Yu-Min Zhang, Teng-Kun Li, Rui Xiong and Ke Xu
- 047501 Nanofabrication of 50 nm zone plates through e-beam lithography with local proximity effect correction for x-ray imaging**
Jingyuan Zhu, Sichao Zhang, Shanshan Xie, Chen Xu, Lijuan Zhang, Xulei Tao, Yuqi Ren, Yudan Wang, Biao Deng, Renzhong Tai and Yifang Chen
- 047503 Magnetocaloric effect and critical behavior of the Mn-rich itinerant material Mn_3GaC with enhanced ferromagnetic interaction**
Pengfei Liu, Jie Peng, Mianqi Xue and Bosen Wang
- 047701 Improvement of memory characteristics by employing a charge trapping layer with combining bent and flat energy bands**
Zhen-Jie Tang, Rong Li and Xi-Wei Zhang
- 047801 Refractive index of ionic liquids under electric field: Methyl propyl imidazole iodide and several derivatives**
Ji Zhou, Shi-Kui Dong, Zhi-Hong He and Yan-Hu Zhang
- 047802 Dependence of limited radiative recombination rate of InGaN-based light-emitting diode on lattice temperature with high injection**
Jiang-Dong Gao, Jian-Li Zhang, Zhi-Jue Quan, Jun-Lin Liu and Feng-Yi Jiang
- INTERDISCIPLINARY PHYSICS AND RELATED AREAS OF SCIENCE AND TECHNOLOGY**
- 048102 A numerical study of dynamics in thin hopper flow and granular jet**
Meng-Ke Wang, Guang-Hui Yang, Sheng Zhang, Han-Jie Cai, Ping Lin, Liang-Wen Chen and Lei Yang
- 048103 Moisture-sensitive torsional cotton artificial muscle and textile**
Yuanyuan Li, Xueqi Leng, Jinkun Sun, Xiang Zhou, Wei Wu, Hong Chen and Zunfeng Liu
- 048104 Characteristics of AlGaIn/GaN high electron mobility transistors on metallic substrate**
Minglong Zhao, Xiansheng Tang, Wenxue Huo, Lili Han, Zhen Deng, Yang Jiang, Wenxin Wang, Hong Chen, Chunhua Du and Haiqiang Jia
- 048502 Investigation of active-region doping on InAs/GaSb long wave infrared detectors**
Su-Ning Cui, Dong-Wei Jiang, Ju Sun, Qing-Xuan Jia, Nong Li Xuan Zhang, Yong Li, Fa-Ran Chang, Guo-Wei Wang, Ying-Qiang Xu and Zhi-Chuan Niu
- 048503 Dark count in single-photon avalanche diodes: A novel statistical behavioral model**
Wen-Juan Yu, Yu Zhang, Ming-Zhu Xu and Xin-Miao Lu
- 048504 Stackable luminescent device integrating blue light emitting diode with red organic light emitting diode**
Kang Su, Jing Li, Chang Ge, Xing-Dong Lu, Zhi-Cong Li, Guo-Hong Wang and Jin-Min Li
- 048505 A method of generating random bits by using electronic bipolar memristor**
Bin-Bin Yang, Nuo Xu, Er-Rui Zhou, Zhi-Wei Li, Cheng Li, Pin-Yun Yi and Liang Fang

- 048701 Structural and thermal stabilities of Au@Ag core-shell nanoparticles and their arrays: A molecular dynamics simulation**
Hai-Hong Jia, De-Liang Bao, Yu-Yang Zhang and Shi-Xuan Du
- 048702 Effect of C₆₀ nanoparticles on elasticity of small unilamellar vesicles composed of DPPC bilayers**
Tanlin Wei, Lei Zhang and Yong Zhang
- 048703 Electron beam irradiation on novel coronavirus (COVID-19): A Monte-Carlo simulation**
Guobao Feng, Lu Liu, Wanzhao Cui and Fang Wang
- 048801 Two-step processed efficient perovskite solar cells via improving perovskite/PTAA interface using solvent engineering in PbI₂ precursor**
Cao-Yu Long, Ning Wang, Ke-Qing Huang, Heng-Yue Li, Biao Liu and Jun-Liang Yang
- 048901 Network correlation between investor's herding behavior and overconfidence behavior**
Mao Zhang and Yi-Ming Wang
- 048902 Identifying influential spreaders in complex networks based on entropy weight method and gravity law**
Xiao-Li Yan, Ya-Peng Cui and Shun-Jiang Ni

JUST FOR AUTHORS
— CHINESE PHYSICS B